Nigerian Journal of Engineering
Faculty of Engineering
Ahmadu Bello University
Samaru-Zaria, Nigeria

Vol. 26, No. 2, August 2019
ISSN: 0794 - 4756

SYNTHESIS AND CHARACTERIZATION OF PLATINUM-COBALT SUPPORTED ON ACTIVATED CARBON ELECTROCATALYST

S. Magaji[1, 2], A. Hamza[2] and B. Mukhtar[*2]

[1]Ibrahim Shehu Shema Center for Renewable Energy Research, Umaru Musa Yar'adua University Katsina, Nigeria
[2]Department of Chemical Engineering, Ahmadu Bello University, Zaria, Nigeria
[*]Corresponding Author's Email: bmukhtar@abu.edu.ng; belloonline@yahoo.co.uk

ABSTRACT
Activated carbon (AC) was produced from coconut shell using phosphoric acid as an activating agent. It was characterized using X-ray diffraction (XRD), Scanning electron micrographs (SEM), Fourier transform infrared spectra (FTIR), Brunauer-Emmett-Teller (BET) and Electrical conductivity test (EC) techniques. The XRD results showed that the AC has graphitic structure while the SEM images revealed formation of pores on the AC. The FTIR spectra revealed that chemical transformation has taken place during carbonization and chemical activation, the BET results showed a specific surface area of $3927400\ cm^2/g$*, pore size of 3.1nm and pore volume of* $0.15\ cm^3/g$ *while the EC of the AC was found to be 0.025 S/cm. Pt and Pt-Co alloys with different Pt/Co ratios supported on the activated carbon were synthesized by impregnation-reduction method. The synthesized electrocatalysts were characterized by XRD, BET and EC methods. The XRD analysis confirmed the formation of Pt-Co alloy on the activated carbon and a decrease of metal particle size and lattice parameter with increase in the cobalt content. The BET results for the electrocatalysts showed the reduction in the surface area as the percentage of Pt and Co deposited on the activated carbon increased. The EC increased as the percentage of the active species deposited on the activated carbon increased. Comparative analysis of the properties of the synthesized electrocatalyst and reported electrocatalysts in the literature showed that the prepared Pt-Co/ACelectrocatalyst can be used for the methanol electro-oxidation reaction at the anode of the direct methanol fuel cell.*
Keywords: *Platinum, Cobalt, Activated Carbon, Electrocatalyst, Direct Methanol Fuel Cell.*

INTRODUCTION
Direct methanol fuel cell (DMFC) is a low temperature fuel cell ($< 200℃$) which uses liquid methanol as fuel. The advantages of using methanol fuel are ease of handling, it is liquid at room temperature and has a high energy density (Prabhuram *et al.,* 2007). Bimetallic Pt-Ru is considered to be the most active electrocatalyst for the methanol electro-oxidation reaction at the anode of the direct methanol fuel cell due to its bi-functional mechanism and ligand (electronic) effect (Celorrio *et al.,* 2013; Huajie *et al.,* 2012). However, the scarcity (making it expensive) of ruthenium and its toxicological effect remain problematic.

Therefore, investigations on less costly alloys containing platinum and non-noble metals (which are mostly cheaper) have attracted researchers' interest. Among the diverse bimetallic electrocatalysts containing non-noble metals developed, Pt-Co alloy has been reported to have high performance for the methanol electro-oxidation reaction under the commonly used acidic conditions *(Huajie et al.,* 2012).

The significant improvement in the electrocatalytic activities of the Pt-Co systems is attributed to the fact that cobalt is more electropositive than platinum. Thus, Pt could withdraw electrons from the immediate cobalt atoms, leading to improved C-H cleavage reaction and the presence of cobalt oxide offers an oxygen source for CO oxidation at lower potentials (Huajie *et al.,* 2012).

Several materials have been used as electrocatalyst support because they have appropriate support properties, inertness toward unwanted reactions and stability under regeneration and reaction conditions, adequate mechanical properties, electrical conductivity, modifiable surface area and good porosity. Activated carbon produced from coconut shell showed similar stable physical properties and larger surface area (La´zaro *et al.,* 2015).This paper reports synthesis and characterization of activated carbon supported platinum-cobalt electrocatalyst for potential application in the methanol electrooxidation reaction at the anode of the direct methanol fuel cell.

MATERIALS AND METHOD
Materials
Hexachloroplatinic (IV) hexahydrate (39 % of Pt), cobalt (II) chloride hexahydrate (98%), sodium borohydride (90%), potassium hydroxide (98%) and phosphoric acid (85%) were purchased from Cardinal Scientific Supplies, Zaria-Nigeria. Activated carbon was prepared from *Cocos nucifera* specie of coconut shell. All chemicals were used as received without further purification. Distilled water was used in the solution preparation.

Preparation of activated carbon from coconut shell
The Coconut shell sample was cleaned with deionized water and dried in an oven at 110℃ for 48 h to reduce moisture content (Song *et al.,* 2014). The dried sample was crushed using mortar and pestle and sieved to a range of 125 µm. 60 g of the sample was weighed and inserted using tongs into furnace for carbonization. The tubular furnace was set to a temperature of 600℃ (Diao *et al*., 2002 and Mukhtar *et al*., 2015) under Nitrogen with flow rate of 150 ml/min and held for 1h. 20 g of the carbonized sample was weighed into a beaker and activated with 85% w/w H3PO4 in the ratio 1:1 to form a paste. The soaking period was 24h and the sample was neutralized using 1 M KOH to remove the acid. Washing was

carried out until the pH was 7 and finally, the sample was dried in an oven at 110℃ for 24 h.

Synthesis of Pt/AC and Pt-Co/AC electrocatalyst

The Pt-Co/ACelectrocatalyst with a loading of 10 wt. % Pt and Pt-Co (20 wt. %, 30 wt. %, 40 wt. %) supported on activated carbon produced from coconut shell were synthesized using $NaBH_4$ as a reducing agent at room temperature. Appropriate amount of the activated carbon was mixed with distilled water and stirred for 1h, then metal precursors ($H_2PtCl_6.6H_2O$ and $CoCl_2.\ 6H_2O$) were added to the mixture and stirred for 2h. Appropriate amount of $NaBH_4$ based on the stoichiometry of Pt and Co to $NaBH_4$ ratio of 1:70 was used (Amin *et al.,* 2011). The sodium borohydride solution was added drop-wise to the mixture and stirred for 3h to complete reduction of the metals. Finally, the mixture was filtered and washed at least six times to remove a chloride ion (which was confirmed using the silver nitrate test) and then dried at 80℃ for 8h.

Physical characterization of the support and the electrocatalyst

Powder X-ray diffraction study

XRD patterns were obtained using PAN analytical/ Empyrean diffractometer equipment using $Cu-K\propto$ as the radiation source ($\boldsymbol{\lambda}$ = 0.15056 nm), operating under a voltage of 45 Kv and current of 25 mA. The diffraction angle (2θ) was varied from 15° to 85°.

SEM analysis

The morphological study of the raw coconut shell, carbonized coconut shell and the activated carbon produced from coconut shell were done using Phenom Pro-X scanning electron microscope.

FTIR spectrum study

The surface chemistry of the raw coconut shell and the activated carbon were analyzed by identifying the surface functional groups using Fourier Transform Infrared Spectrometer (FTIR-630) by Agilent Technology.

BET measurement

Nitrogen adsorption at 77 K was carried out using Quantachrome Novawin instrument to obtain the adsorption isotherm of the samples. The specific surface areas of the porous carbon were determined by nitrogen adsorption data in relative pressure range from 0.05 to 0.3 using Brunauer-Emmett-Teller (BET) method. All samples were out gassed at 250℃ for 3 h prior to analysis.

Electrical conductivity measurement

The powder samples of Ac and different ratio of Pt-Co/AC were pelletized to form cylindrical shape using a compressing machine. The thickness and diameter of the pelletized samples were measured using a micro-meter screw gauge and venire caliper, respectively. The radius of the samples was calculated using Equation 1.

$$r = \frac{d}{2} \quad (1)$$

The areas of the samples were calculated using Equation 2.

$$A = \pi r^2 \quad (2)$$

The resistance of the samples was measured using programmable LRC-meter Bridge. The resistivity was obtained using Equation 3.

$$\rho = \frac{RA}{L} \quad (3)$$

where, ρ is the resistivity, R is the resistance, L is the thickness and A the cross sectional area. The electrical conductivity was obtained by taking the inverse of the resistivity (i.e. Equation 3).

$$\sigma = \frac{1}{\rho} \quad (4)$$

RESULTS AND DISCUSSION

Activated carbon yield

The activated carbon yield was obtained using Equation 5.

$$Yield = \frac{w_2}{w_o} * 100 \quad (5)$$

where, w_o is the original mass of the precursor on a dry basis and w_2 is the mass of the carbonaceous material after activation, washing and drying.

Table1 shows the comparison of the yield of the various AC produced from different sources using different methods of preparation. It can be observed from the table that the activated carbon produced from coconut shell using chemical activation method has percentage yield of 24.6%, which is higher than that produced from corn cobs, nut shell, cherry stone and apricot stone produced using steam pyrolysis method of preparation.

Table 1: Comparison of the activated carbon yield from different sources

Carbon source	Condition of preparation	Activated carbon yield (%)	References
Coconut shell	Chemical activation 600℃	24.6	Present work
Peanut hulls	Chemical activation 500℃	22.0	(Girgis *et al.,* 2002)
Corn cobs	Chemical activation 500℃	18.3	(El-Hendawy *el al.,* 2001)
Grain sorghum	Chemical activation 600℃	26.0	(Diao *et al.,* 2002)
Almond shell	Chemical activation*	24.0	(Ahmedna *et al.,* 2004)
Corn cobs	Steam pyrolysis 700℃	20.1	(El-Hendawy *el al.,* 2001)
Nut shell	Steam pyrolysis 800℃	17.9	(Savova *et al.,* 2001)
Cherry stone	Steam pyrolysis 800℃	11.2	(Savova *et al.,* 2001)
Apricot stones	Steam pyrolysis 800℃	18.2	(Savova *et al.,* 2001)

* Activation temperature not indicated

Surface morphology of the support

The scanning electron micrographs of raw coconut shell, carbonized coconut shell and the activated carbon are illustrated in plate 1(a), 1(b) and 1(c) respectively. The SEM of raw coconut shell revealed that the surface was curly-form resulting from the existence of cellulose, hemicelluloses and lignin in the raw material (Shamsuddin *et al.*,2016). Plate.1 (b) shows the SEM image of carbonized coconut shell and formation cracks due to the elimination of non-carbon materials during carbonization process while Plate. 1(c) shows the SEM image of the activated carbon after the activation with H_3PO_4.

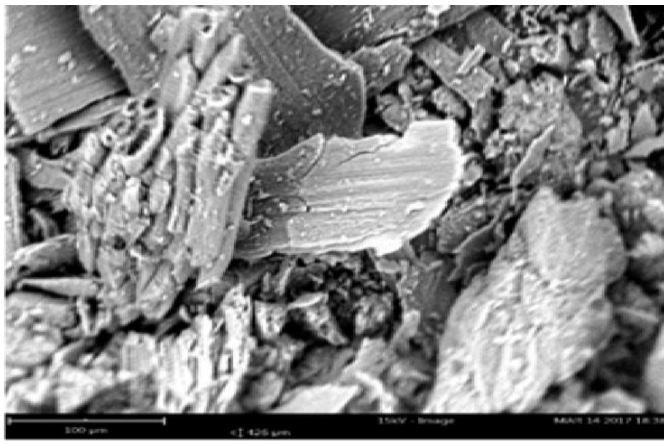

(a)

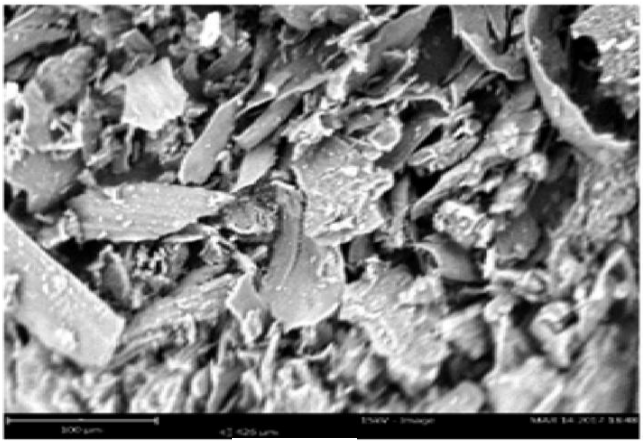

(b)

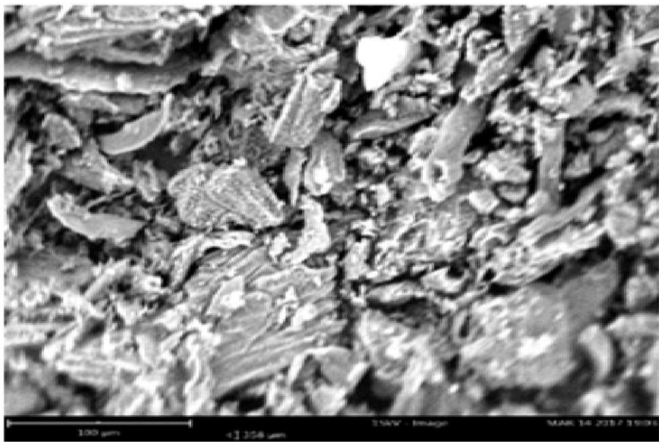

(c)

Plate 1: SEM images (a) Raw coconut shell (b) Carbonized coconut shell (c) Activated carbon

Fourier transform infrared analysis of the support

Infrared spectroscopy was used in this work to acquire information about the functional groups of the carbon material. Figures 1(a) and (b) show the FTIR spectra of raw coconut shell, and the activated carbon. For raw coconut shell, 3362.1 cm^{-1} band indicate O-H stretching vibrations in alcohols and adsorbed water (Hadoun *et al.,* 2013). The raw coconut shell characteristics band at 2896.1 cm^{-1} allocated to C-H stretching indicates methyl and methylene groups. Band at 17220 cm^{-1} indicates C=O stretching of the acetyl group in hemicellulose (Shamsuddin *et al.,* 2016). Also bands at 1595.3, 1505.8, 1457.4 and 1420.1 cm^{-1} of the raw coconut shell are due to the skeletal C=C vibrations of aromatic rings. 1371.7cm^{-1} band indicate stretching vibrations of $–CH_3$ of methyl structures (Hadoun *et al.,* 2013). Bands at 1326.9 cm^{-1} and 1230 cm^{-1} are indicative of N-O and C-O stretching vibration respectively (Shamsuddin *et al.,* 2016). Band at 1162.9 cm^{-1} represent C-O stretching of vibration in the alcohols. Band at 1028.7 cm^{-1} is attributed to C-O-C asymmetrical axial deformation of ethers (Hadoun *et al.,* 2013). Bands at 767.8 cm^{-1} and 697 cm^{-1} are due to out-of-plane deformation mode of C-H for different substituted benzene rings (Yakout and El-deen, 2012). From the spectrum it can be observed that the main oxygen functional groups present in the raw coconut shell are carbonyl, ethers and alcohol groups which are normally present in plant cellulose (Shamsuddin *et al.,* 2016).

The disappearance of peaks in Figure:1b of the activated carbon at the bands 2896.1 cm^{-1}, 1722 cm^{-1}, 1595.3 cm^{-1} ,1505.8 cm^{-1}, 1457.4 cm^{-1} ,1420.1 cm^{-1} ,1326.9 cm^{-1} and 1230 cm^{-1} indicate breakdown of functional groups present in oxygenated hydrocarbons, replicating the carbohydrate structure of cellulose and hemi-cellulose (Shamsuddin *et al.,* 2016). The band at 2653.9 cm^{-1} in the activated carbon (Figure 1 (b)) indicates O-H stretching vibration of the carboxylic acid group.

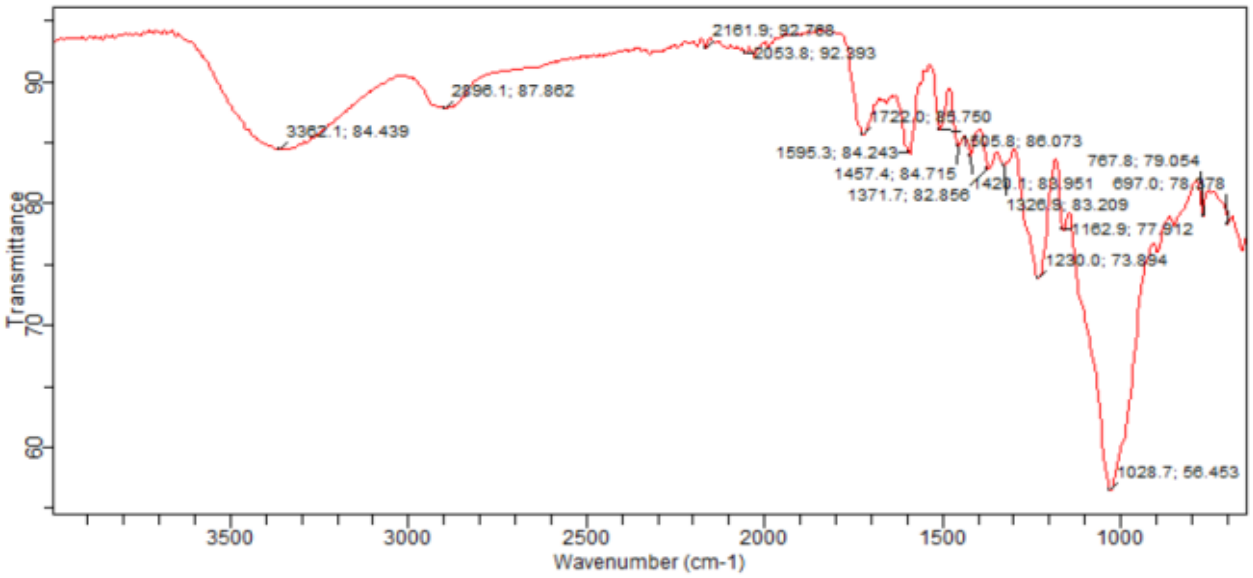

(a)

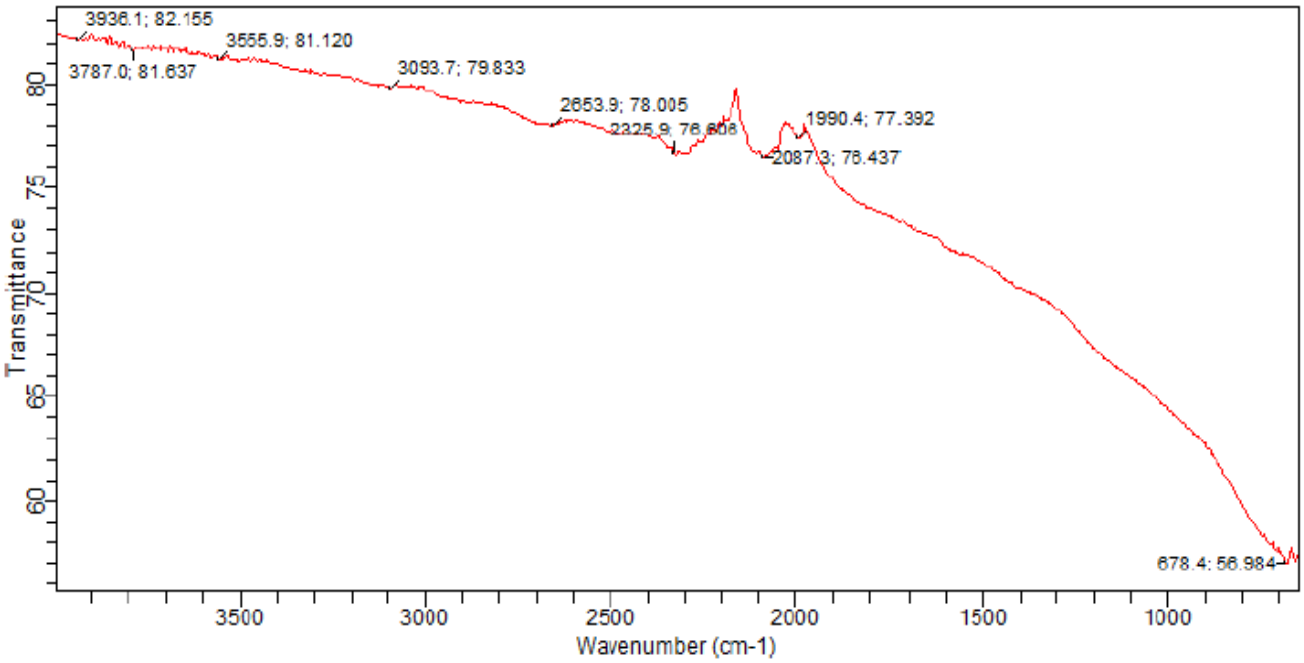

(b)

Figure 1: FT-IR Spectra, (a) Raw coconut shell, (b) Activated carbon

Specific surface area analysis of the activated carbon

The multipoint BET method was used to calculate the specific surface areas, while the Dubinin - Radushkevich (DR) method was used to estimate the pore volume and pore size. Table 2 gives the BET analysis result of the activated carbon produced from coconut shell. The specific surface area and the average pore size were found to be 392.740 m^2/g and 3.1 nm, respectively. The average pore size value indicates that it is a mesoporous material.

Table 2: Surface area analysis of the activated carbon produced from coconut shell

Specific surface area	392.740 m^2/g
Average pore size	3.1 nm
Pore volume	0.15 cm^3/g

XRD analysis

Figure 2 shows the XRD patterns of the AC, 10 wt.% Pt/AC, 20 wt.% Pt-Co/AC-1, 30wt.% Pt-Co/AC-2 and 40 wt.% Pt-Co/AC-3 electrocatalyst samples for the 2θ range of 15° to 85°.The activated carbon revealed characteristics diffraction peaks at 2θ = 26.6°and 43.6°. These peaks can be ascribed to the hexagonal graphite structures of carbon (002) and (100), (JCPDS, card No. 41-1487) respectively, (Amin *et al.*, 2011; Li *et al.*, 2003) .The peak at 2θ= 26.6° is observed in Pt/AC, Pt-Co/AC-1 and Pt-Co/AC-2 indicating the presence of the activated carbon. However, it is nearly absent in Pt-Co/AC-3 which indicate the complete coverage of the carbon surface by Pt-Co particles. Also, the pattern of the Pt/AC revealed diffraction peaks of (111), (200), (220) and (311) (JCPDS, card 4-802) at 2θ values of 39.8°,46.3°,67.8° and 81.6°, respectively. These peaks indicate that Pt is present in the face-centered cubic (FCC) structure, which is similar to the observation by Chen *et al.*(2015), Angelucci *et al.* (2007) and Zeng and Lee (2005). The diffraction peaks of Pt-Co/AC-1, Pt-Co/AC-2 and Pt-Co/AC-3 showed similar pattern to those of Pt, except the 2θ values were shifted to higher values which increased with increase in the Co content. This indicate lattice contraction due to the incorporation of smaller Co atoms into the FCC crystal structure of Pt and formation Pt-Co alloy (Huajie *et al.*, 2012). The metallic Co or its oxides peaks were absent, but their presence cannot be ignored because they are present in a very small amount or even in an amorphous form (Amin *et al.*, 2011; Huajie *et al.*, 2012).

(a) Ac (b) Pt/AC (c) Pt-Co/AC-1 (d) Pt-Co/AC-2 (e) Pt-Co/AC-3

The lattice parameter(a_{fcc}) and average particle size for all materials were calculated from the (220) diffraction peaks (Chen e*t al.*, 2015; Hernández-Fernández *et al.*, 2010; Prabhuram *et al.*, 2007). The average particle size for all the catalyst is calculated using the Debye-Scherrer Equation (Li *et al.*, 2003; Zeng and Lee, 2005):

$$L = \frac{0.9\,\lambda_{Cuk\alpha}}{B_{2\theta}\cos\theta_{max}} \quad (6)$$

where, L is the average particle size, $\lambda_{Cuk\alpha}$ is the X-ray wavelength used (0.15406nm for Cu kα), θ_{max} is the maximum angle of the (220) peak and $B_{2\theta}$ is the half peak width for Pt (220) in radians.

The average size of platinum particles calculated from Pt (220) peak was estimated to be 9.88 nm, 8.69 nm, 8.05 nm and 6.71 nm for Pt/AC, Pt-Co/AC-1, Pt-Co/AC-2 and Pt-Co/AC-3 electrocatalyst samples, respectively. This shows that the increment of Co content led to reduction in the average catalyst particle size. The reduction in intensity and broadening nature of the diffraction peaks of Pt-Co/AC-3 catalyst replicate its smallest particle size (6.71 nm) among the Pt-Co/AC electrocatalysts.

The lattice parameter (a_{fcc}) values for the catalyst were calculated using (220) diffraction peaks (Angelucci *et al.*, 2007).

$$a_{fcc} = \frac{\sqrt{2}\lambda_{Cuk\alpha}}{\sin\theta_{max}} \quad (7)$$

where, a_{fcc} is the lattice parameter, $\lambda_{Cuk\alpha}$ is the X-ray wavelength used (0.15406 nm for Cu kα), θ_{max} is the maximum angle of the (220) peak. The lattice parameters calculated are 0.3906, 0.3863, 0.3859 and 0.3848 for Pt/AC, Pt-Co/AC-1, Pt-Co/AC-2 and Pt-Co/AC-3, respectively.

Assuming that the dependence of the lattice parameter is the same for supported and unsupported Pt-Co alloys, the percentage of atomic cobalt present in Pt-Co alloy is calculated using Equation 4 (Salgado *et al.*, 2004).

$$a_{fcc} = a_o - kX_{Co} \quad (8)$$

where, $a_o = 0.392$ nm is the lattice parameter for pure platinum supported on carbon and $k = 0.0368$ nm is a constant(Salgado *et al.*, 2004). The result of calculated values of X_{Co} using Equation 8 are included in Table 3.

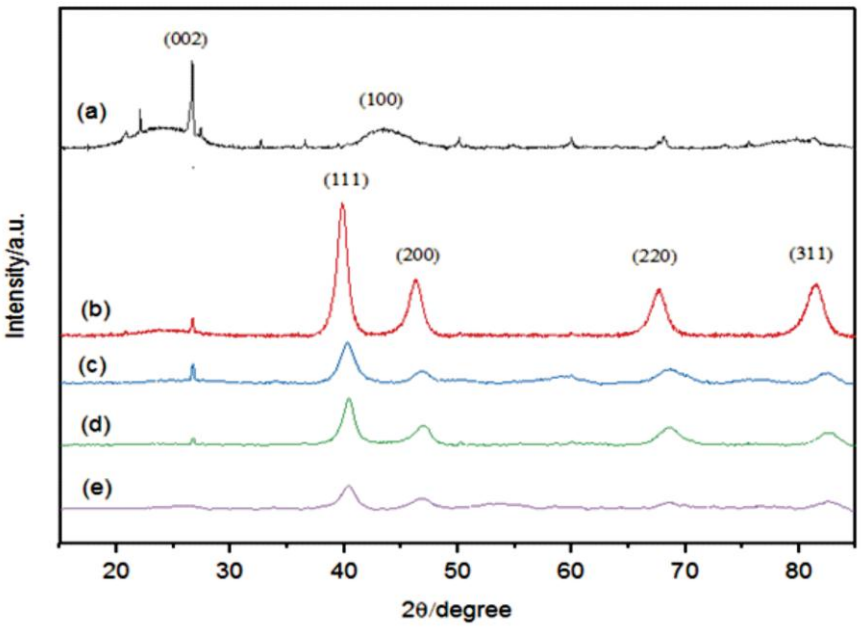

Figure 2: XRD patterns of the prepared Ac and electrocatalysts

Table 3: The particle size and lattice parameter of the prepared electrocatalysts

Electro-catalysts	**(220) Peak**	**Average particle size (nm)**	**Lattice Parameter (nm)**	**X_{Co} Calculated from Equation (8)**
Pt/Ac	67.80	9.88	0.3906	-
Pt-Co/Ac-1	68.67	8.69	0.3863	0.1169
Pt-Co/Ac-2	68.74	8.05	0.3859	0.1277
Pt-Co/Ac-3	68.98	6.71	0.3848	0.1576

Specific surface area of the activated carbon

A comparison of the surface area and pore volume of the electrocatalyst support of the activated carbon produced from coconut shell of the present work with other literature reported values of the electrocatalyst support produced from different sources are listed in Table 4. It can be observed from the data provided in the table that the BET surface area due to the current study $(392.740 * 10\text{^}4\ cm^2/g)$ is higher than that of CNC$(124\ cm^2/g)$, CNF $(96 * 10^4 cm^2/g)$, Vulcan XC-72R $(218 * 10^4\ cm^2/g)$, GNF $(10 - 200 * 10^4\ cm^2/g)$, fall within the range of MWNT $(200 - 400 * 10\text{^}4\ cm^2/g)$ and approximately equal to that of CMK-3$(400 * 10^4\ cm^2/g)$. It can also be observed from the data provided in the table that the pore volume due to the present study (0.15 cm^3/g), is equal to that of CXG (0.15 cm^3/g), slightly lower than that of CNC (0.16 cm^3/g), and fall within the range of that of SWNT (0.15-0.3 cm^3/g). We can conclude that base on the surface area and pore volume the activated carbon produced from coconut shell due to the present work can be used as catalyst support for the anode of direct methanol fuel cell application where, CNC: Carbon nanocoil, CNF: Carbon nanofiber, CXG: Mesoporous Carbon Xerogel , SWNT: Single-walled nanotubes, MWNT: Multi-walled nanotube. GNF: Graphite nanofiber, CMK-3: Ordered Mesoporous Carbon.

Table 4: Comparative analysis of the produced AC with other electrocatalyst support materials

Catalyst support	**Surface area $(cm^2/g) * 10^6$**	**Pore volume (cm^3/g)**	**References**
Activated carbon	3.9	0.15	Present work
CNC	1.2	0.16	Calvillo *et al.*, 2013
CNF	0.96	0.23	Calvillo *et al.*, 2013
Vulcan XC-72R	2.2	0.41	Calvillo *et al.*, 2013
CXG	5.3	0.15	Alegre *et al.*, 2014
SWNT	4-9	0.15-0.3	Serp *et al.*, 2003
MWNT	2-4	0.5-2	Serp *et al.*, 2003
GNF	0.1-2	0.5-2	Serp *et al.*, 2003
CMK-3	4	0.273	Salgado *et al.*, 2010

Electrical conductivity of the activated carbon support

A comparison of the electrical conductivity of the activated carbon produced from coconut shell of the present work with some literature reported values of electrocatalyst support are listed in Table 5. It can be observed from the data provided in the table that the electrical conductivity of the synthesized activated carbon (0.025 S/cm) falls within the range of that of OMC (0.003-1.4 S/cm) and lower than that of CNH, CNF, Vulcan XC-72R, CXG, SWNT, MWNT and BDD. One of the properties of a good support material for an electrocatalyst is sufficient electrical conductivity to conduct electrons effectively. Therefore, there is need to increase the electrical conductivity of the synthesized activated carbon (for example by blending with carbon nano fiber or graphene), which will lead to a better performance of the electrocatalysts for fuel cell application.

Comparative analysis of the produced electrocatalysts

A comparison of the properties of the various electrocatalysts synthesized using AC from coconut shell as a support in the present work with other literature reported properties of electrocatalyst supported on various materials is reported in Table 6. Pt/AC and different loadings of Pt-Co/AC electrocatalysts were prepared, that is 10 wt.% Pt/AC, 20 wt.% PtCo/AC-1, 30 wt.% PtCo/AC-2 and 40 wt.% PtCo/AC-3. It can be observed from the data provided in Table 6 that the BET specific surface area decreased as the percentage of the active species deposited on to the activated carbon increased. This indicates that the pores of the activated carbon support material are occupied by Pt and Co active species deposited on the support and as the percentage of the active species deposited increased more pores were occupied which led to the reduction in specific surface area of the electrocatalysts. It can also be observed from the data in Table 6 that, the average particle size decreased as the percentage of the active species deposited onto the support increased this is due to the incorporation of small cobalt atom into FCC crystal structure of platinum. These results are supported by those obtained by Amin *et al.* (2012), that prepared Pt-NiO/C electrocatalysts and found that the presence of NiO led to the formation of smaller average particle size of the electrocatalysts. In addition, Angelucci *et al.* (2007), prepared Pt-Ru/C electrocatalysts and observed a reduction of metal average particle size with increase in Ru content.

Table 5: Comparative analysis of EC of different catalysts support

Catalyst support	**Electrical conductivity (S/cm)**	**References**
Activated carbon	0.025	Present work
CNH	3-200	Antolini and Gonzalez, 2009
CNF	10^2-10^4	Antolini and Gonzalez, 2009

Vulcan XC-72R	4	Antolini and Gonzalez, 2009
CXG	>1	Antolini and Gonzalez, 2009
SWNT	$10\text{-}10^{4}$	Antolini and Gonzalez, 2009
MWNT	0.3-3	Antolini and Gonzalez, 2009
OMC	$0.3*10^{-2}\text{-}1.4$	Antolini and Gonzalez, 2009
BDD	1.5	Antolini and Gonzalez, 2009

Table 6: Comparative analysis of the produced electrocatalysts with other electrocatalysts

Electrocatalyst	**BET surface area (m^2/g)**	**XRD particle size (nm)**	**References**
Pt/AC	199.661	9.88	Present work
Pt-Co/AC-1	198.468	8.69	Present work
Pt-Co/AC-2	180.709	8.05	Present work
Pt-Co/AC-3	165.708	6.71	Present work
Pt/CMK-3	62	4.5	Salgado *et al.*, 2010
Pt/C	-	9.8	Amin *et al.*, 2012
Pt/Vulcan	-	10.1	Angelucci *et al.*, 2007
Pt-Ru/Vulcan	51	6.39	Carmo *et al.*, 2005
Pt-Ru/CMK-3	92	3.2	Salgado *et al.*, 2010
Pt-NiO/C	-	4.9	Amin *et al.*, 2012

Electrical conductivity of the produced electrocatalysts

Figure 3 shows the electrical conductivity of the synthesized AC, 10 wt % Pt/AC, 20 wt % Pt-Co/AC-1, 30 wt % Pt-Co/AC-2 and 40 wt % Pt-Co/AC-3 as a function of metal content on the Ac support. It can be observed from the figure that the electrical conductivity increased as the loading of the active species increased. The electrical conductivity is dependent on the morphological characteristics (such as average particle size, loading and dispersion of the active species on the support) of the electrocatalyst (Grinou et al., 2012). The electrical conductivity of Pt-Co/AC-3 is higher than that of Pt-Co/AC-2, Pt-Co/AC-1, Pt/AC and AC because of its smaller average particle size of 6.71 nm, high loading of the metal and good dispersion of the active species on the synthesized activated carbon support material, while the low electrical conductivity of Pt/AC, Pt-Co/AC-1, and Pt-Co/AC-2 may be due to insufficient electrical contact point probably because of agglomeration of the active species dispersed over the AC support.

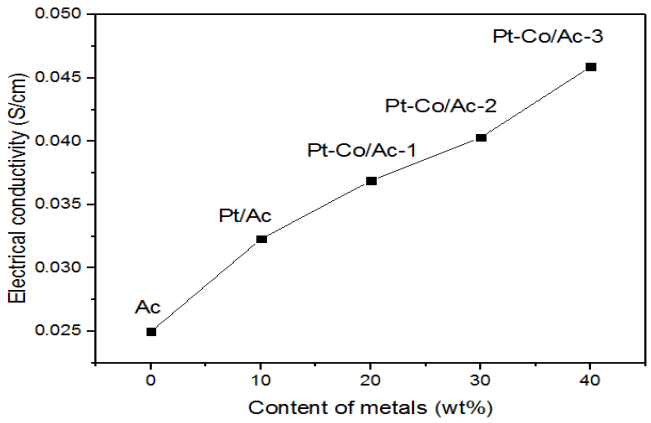

Figure 3: Effect of catalyst loading on the AC on the electrical conductivity of the synthesized electrocatalysts

CONCLUSIONS

Activated carbon was prepared from *Cocos nucifera* specie of coconut shell using chemical activation method and used as electrocatalyst support. Pt and different loading of Pt-Co were dispersed over the activated carbon support using $NaBH_4$ as the reducing agent. The XRD result showed successful impregnation of the active species on the activated carbon support and formation of Pt-Co alloy. The BET result for the electrocatalysts showed the reduction in area as the loading of Pt and Co dispersed over the support increased. The electrical conductivity of the synthesized electrocatalyst increased as the percentage of the metal content increased. Pt-Co/AC-3 was found to have highest electrical conductivity among the prepared electrocatalysts. The comparative analysis of the synthesized electrocatalysts due to the present study with the reported electrocatalysts indicated that the prepared electrocatalysts can be used at the anode of direct methanol fuel cell for the methanol electro-oxidation reaction.

ACKNOWLEDGEMENT

Suleiman Magaji is grateful for the study fellowship awarded to him by the Umaru MusaYar'adua University, Katsina.

REFERENCES

Ahmedna, M., Marshall, W. E., Husseiny, A. A. and Rao, R. M. (2004). The use of nutshell carbons in drinking water filters for removal of trace metals. *Water Research*, *38*, 1062–1068.

Alegre, C., Gálvez, M. E., Moliner, R., Baglio, V., Aricò, A. S. and Lázaro, M. J. (2014). Towards an optimal synthesis route for the preparation of highly mesoporous carbon xerogel-supported Pt catalysts for the oxygen reduction reaction. *Applied Catalysis B: Environmental*, *147*, 947–957.

Amin, R. S., El-Khatib, K. M., Hameed, R. M. A., Souaya, E. R. and Etman, M. A. (2011). Synthesis of Pt-Co nanoparticles on multi-walled carbon nanotubes for methanol oxidation in H2SO4 solution. *Applied Catalysis A: General*, *407* (1–2), 195–203.

Amin, R. S., Hameed, R. M. A., El-Khatib, K. M., Youssef, M. E. and Elzatahry, A. A. (2012). Pt-NiO/C anode electrocatalysts for direct methanol fuel cells. *Electrochimica Acta*, *59*, 499–508.

Angelucci, C. A., D'Villa Silva, M. and Nart, F. C. (2007). Preparation of platinum-ruthenium alloys supported on carbon by a sonochemical method. *Electrochimica Acta*, *52* (25), 7293–7299.

Antolini, E. and Gonzalez, E. R. (2009). Polymer supports for low-temperature fuel cell catalysts. *Applied Catalysis A: General*, *365* (1), 1–19.

Calvillo, L., Celorrio, V., Moliner, R., Garcia, A. B., Caméan, I. and Lazaro, M. J. (2013). Comparative study of Pt catalysts supported on different high conductive carbon materials for methanol and ethanol oxidation. *Electrochimica Acta*, *102*, 19–27.

Carmo, M., Paganin, V. A., Rosolen, J. M. and Gonzalez, E. R. (2005). Alternative supports for the preparation of catalysts for low-temperature fuel cells: The use of carbon nanotubes. *Journal of Power Sources*, *142* (1–2), 169–176.

Celorrio, V., Calvillo, L., Moliner, R., Pastor, E. and Lazaro, M. J. (2013). Carbon nanocoils as catalysts support for methanol electrooxidation: A Differential Electrochemical Mass Spectrometry (DEMS) study. *Journal of Power Sources*, *239*, 72–80.

Chen, M., Lou, B., Ni, Z. and Xu, B. (2015). PtCo nanoparticles supported on expanded graphite as electrocatalyst for direct methanol fuel cell. *Electrochimica Acta*, *165*, 105–109.

Diao, Y., Walawender, W. P. and Fan, L. T. (2002). Activated carbons prepared from phosphoric acid activation of grain sorghum. *Bioresource Technology*, *81*, 2–9.

El-Hendawy, A. N. A., Samra, S. E. and Girgis, B. S. (2001). Adsorption characteristics of activated carbons obtained from corncobs. *Colloids and Surfaces A: Physicochemical and Engineering Aspects*, *180* (3), 209–221.

Girgis, B. S., Yunis, S. S. and Soliman, A. M. (2002). Characteristics of activated carbon from peanut hulls in relation to conditions of preparation. *Materials Letters*, *57* (1), 164–172.

Grinou, A., Yun, Y. S., Cho, S. Y., Park, H. H. and Jin, H. J. (2012). Dispersion of Pt nanoparticle-doped reduced graphene oxide using aniline as a stabilizer. *Materials*, *5* (12), 2927–2936.

Hadoun, H., Sadaoui, Z., Souami, N., Sahel, D. and Toumert, I. (2013). Characterization of mesoporous carbon prepared from date stems by H_3PO_4 chemical activation. *Applied Surface Science*, *280*, 1–32.

Hernández-Fernández, P., Montiel, M., Ocón, P., Fierro, J. L. G., Wang, H., Abruña, H. D. and Rojas, S. (2010). Effect of Co in the efficiency of the methanol electrooxidation reaction on carbon supported Pt. *Journal of Power Sources*, *195* (24), 7959–7967.

Huajie, H., Dongping, S. U. N. and Xin, W. (2012). PtCo alloy nanoparticles supported on graphene nanosheets with high performance for methanol oxidation. *Chin Sci Bull*, *57* (23), 3071–3079.

Lazaro, M. J., Ascaso, S., Perez-Rodriguez, S., Calderon, J. C., Galvez, M. E., Nieto, M. J. and Celorrio, V. (2015). Carbon-based catalysts: Synthesis and applications. *Comptes Rendus Chimie*, *18* (11), 1229–1241.

Li, W., Liang, C., Zhou, W., Qiu, J., Zhou, †, Sun, G., and Xin, Q. (2003). Preparation and characterization of multiwalled carbon nanotube-supported platinum for cathode catalysts of direct methanol fuel cells. *The Journal of Physical Chemistry B*, *107* (26), 6292–6299.

Mukhtar, B., Ameh, A. O. and Tijjani, L. (2015). Tannery effluent wastewater treatment using activated carbon produced from Almond nutshells. *Nigeria Journal of Engineering and Applied Sciences*, (2), 101-107.

Prabhuram, J., Zhao, T. S., Liang, Z. X. and Chen, R. (2007). A simple method for the synthesis of PtRu nanoparticles on the multi-walled carbon nanotube for the anode of a DMFC. *Electrochimica Acta*, *52* (7), 2649–2656.

.

Salgado, J. R C, Alcaide, F., Alvarez, G., Calvillo, L., Lazaro, M. J. and Pastor, E. (2010). Pt-Ru electrocatalysts supported on ordered mesoporous carbon for direct methanol fuel cell. *Journal of Power Sources*, *195* (13), 4022–4029.

Salgado, José R. C., Antolini, E. and Gonzalez, E. R. (2004). Structure and activity of carbon-supported Pt - Co electrocatalysts for oxygen reduction. *Journal of Physical Chemistry B*, *108* (46), 17767–17774.

Savova, D., Apak, E., Ekinci, E., Yardim, F., Petrov, N., Budinova, T. and Minkova, V. (2001). Biomass conversion to carbon adsorbents and gas. *Biomass and Bioenergy*, *21*(2), 133–142. Serp, P., Corrias, M., and Kalck, P. (2003). Carbon nanotubes and nanofibers in catalysis. *Applied Catalysis A: General*, *253* (2), 337–358.

Shamsuddin, M. S., Yusoff, N. R. N. and Sulaiman, M. A. (2016). Synthesis and characterization of activated carbon produced from Kenaf Core fiber using H_3PO_4activation. *Procedia Chemistry*, *19*, 558–565.

Song, C., Wu, S., Cheng, M., Tao, P., Shao, M. and Gao, G. (2014). Adsorption studies of coconut shell carbons prepared by KOH activation for removal of Lead (II) from aqueous solutions, *6*, 86–98.

Yakout, S. M. and Sharaf El-Deen, G. (2016). Characterization of activated carbon prepared by phosphoric acid activation of olive stones. *Arabian Journal of Chemistry*, *9*, S1155–S1162.

Zeng, J. and Lee, J. Y. (2005). Effects of preparation conditions on performance of carbon-supported nanosize Pt-Co catalysts for methanol electro-oxidation under acidic conditions. *Journal of Power Sources*, *14 0* (2), 268–273.

ERRATUM

The statement published in Vol. 26, No. 1, April 2019 page 35 should be **"in case of inequality constraints violations, limits are enforced according to the criteria given in (Sun *et al.*, 1984; Acha *et al.*, 2004)"** not "in case of inequality constraints violations, limits are enforced according to the criteria given in in Equation (6) (Sun *et al.*, 1984; Acha *et al.*, 2004)".